Korea-Australia Rheology Journal
Vol. 13, No. 3, September 2001 pp. 131-139

Coupled approach of analytical and numerical methods for shape prediction in sheet casting process

Kyung Sun Chae[1], Seong Jae Lee[2]*, Kyung Hyun Ahn and Seung Jong Lee
School of Chemical Engineering, Seoul National University, Seoul 151-742, Korea
[1]Agency for Technology and Standards, Kwacheon 427-010, Korea
[2]Department of Polymer Engineering, The University of Suwon, Suwon 445-743, Korea
(Received July 16, 2001; final revision received August 23, 2001)

Abstract

A coupled approach is proposed for the prediction of sheet profile in sheet casting process, which combines one-dimensional analytical method on planar elongational flow region and three-dimensional numerical method on the other region. The strategy is constructed from the observations that the flow domain of sheet casting process can be separated into two parts based on the flow kinematics. The flow field in the central region of sheet, over which the planar elongational flow dominates, is possibly replaced by one-dimensional analytical solution. Then only a partial flow domain near the edge region of sheet, where the flow kinematics cannot be described by the planar elongational flow itself, requires three-dimensional numerical simulation. Good agreement is observed between the coupled approach developed in this study and the full three-dimensional numerical simulation previously developed and reported by the authors. This coupled approach may have provided flexibility with low costs to accommodate a wide range of die sizes in sheet casting process.

Keywords **:** sheet casting process, analytical solution, planar elongational flow, numerical simulation, three-dimensional flow

1. Introduction

The sheet (or film) casting process is an important process for the manufacturing of thin polymer films, such as photographic film, magnetic audio and video tape and food packaging (Werner *et al.*, 1988; Smith and Stolle, 1999). In this process, a polymer is stretched at the exit of the die in order to produce a thin layer of polymer that is cooled in contact with a chill roll. Though the final goal of this process is to produce the sheet having uniform thickness under stable operation conditions, the sheet produced by this process does not show constant thickness profile but shows irregular profile with both edge bead defect and neck-in phenomena in nature. Basic operation procedure of sheet casting process is introduced in the paper previously reported by the authors (Chae *et al.*, 2000). A simplified processing diagram of the process is shown in Fig. 1. As can be easily imagined from the diagram, the two of the most important variables in controlling the sheet thickness seem to be draw ratio and melt drawn length, where the draw ratio is defined as the take-up velocity at the chill roll to the mean velocity of polymer at the exit of the die and the melt drawn length is defined as the length between the exit of the die and the chill roll.

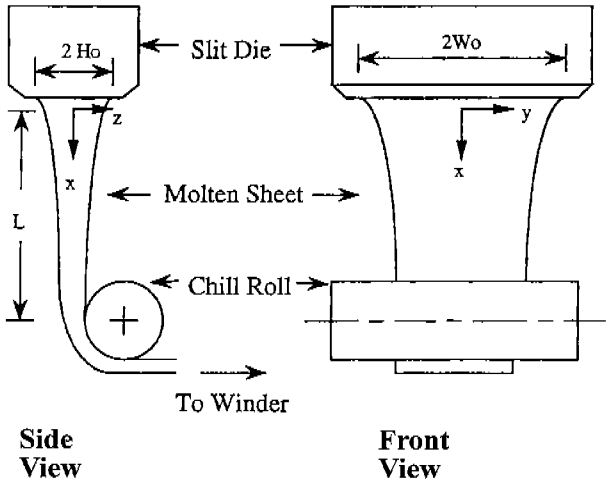

Fig. 1. Schematic diagram of sheet casting process.

Due to the complexity of combined behavior of elongational and shear flows, the prediction of final shape in sheet casting process is only possible through the full

*Corresponding author: sjlee@mail.suwon.ac.kr
© 2001 by The Korean Society of Rheology

three-dimensional numerical simulation. In performing the full three-dimensional simulation on the entire domain of interest within acceptable limits of accuracy, it is inevitable to spend high computational efforts due to large number of unknowns involved. In this process, the width of the sheet as well as the stretching distance are several orders of magnitude larger than the sheet thickness. Consequently, two-dimensional numerical simulations giving a realistic, although incomplete, prediction of the edge bead defect have been developed for a Newtonian fluid (d'Halewyn, 1990; Song, 1993) and for a viscoelastic fluid (Debbaut and Marchal, 1995). When the quasi-elongational approximation is applied on the flow of this process, it is possible to derive a one-dimensional analytical solution. In doing this, several assumptions are required such that the main stream velocity is a function of x alone, and the width and the thickness of the sheet changes slowly along the x direction. In most analyses of sheet casting process, edge effects such as neck-in and edge bead which appear in the edge region are usually neglected. Very recently, the significance of these effects and their dependence on the rheological properties of the melts, the draw ratio, and the extrusion rate was investigated (Canning and Co, 2001). However, it is not unreasonable to assume that the flow kinematics in the central region is not much influenced by the one in the edge region because the width of the sheet is relatively large compared with the thickness and the melt drawn length. Approximately, the flow in sheet casting process can be described as a combination of planar elongational flow near the central region, uniaxial elongational flow along the edge region and combined elongational flow inbetween the two regions. In this study, a one-dimensional approximation is introduced in the flow of central region showing planar elongation where the one-dimensional solution is valid, and a three-dimensional numerical computation is applied in the other region where the approximation is not applicable. The valid range of analytical solutions to predict an accurate sheet profile is determined from a comparison between the one-dimensional approximation and the full three-dimensional numerical solution. This coupled approach which combines the one-dimensional analytical solution of planar elongational flow and the three-dimensional numerical simulation of mixed flow will be applicable to predict the sheet profile in sheet casting process with low computational efforts.

2. One-dimensional solutions of elongational flows

Two types of flows often used to characterize the flows of polymeric liquids are shear flow and elongational (or shearfree) flow (Bird *et al.*, 1987). At first, our attention is restricted to simple flows in which the velocity gradient is independent of position. Simple elongational flows are given by the velocity field:

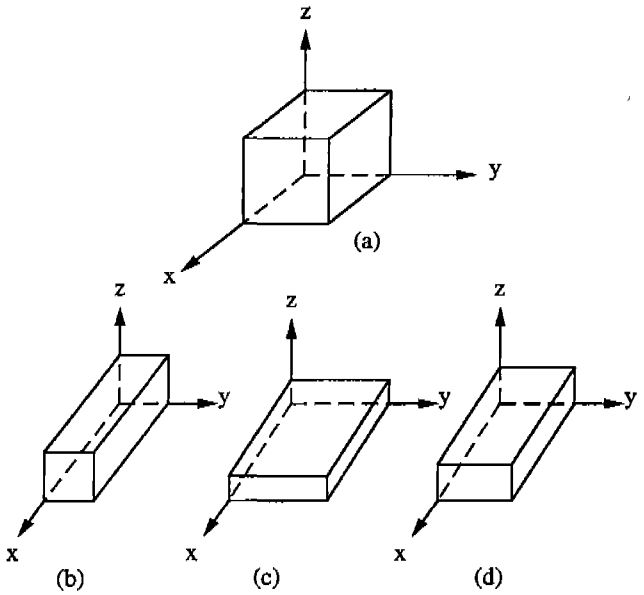

Fig. 2. Simplified illustration of elongational deformations : (a) unit cube, (b) uniaxial elongation, (c) biaxial elongation, (d) planar elongation.

$$u = \dot{\varepsilon}x$$
$$v = -(1-b)\dot{\varepsilon}y \qquad (1)$$
$$w = -b\dot{\varepsilon}z$$

where $0.5 \leq b \leq 1$ and $\dot{\varepsilon}$ is the elongation rate du/dx which depends on time. Special elongational flows can be obtained for particular choices of the parameter b: $b = 0.5$, $\dot{\varepsilon} > 0$ for uniaxial elongational flow; $b = 0.5$, $\dot{\varepsilon} < 0$ for biaxial elongational flow; $b = 1$ for planar elongational flow. The effects of three kinds of elongational flows on a cube of material at steady state are illustrated in Fig. 2. In steady elongational flows, $\dot{\varepsilon}$ is assumed to be independent of time, i.e., it is presumed that $\dot{\varepsilon}$ is constant for such a long time that all the stresses in the fluid are time independent.

One-dimensional equations describing Newtonian film flows were previously derived by earlier investigators (Yeow, 1974; Pearson and Matovich, 1969). Here, we extend their analysis using more general elongational flows, eq (1). Extrudate swell just downstream of the die may be neglected for a thin and long film so that the governing equations can be averaged over the cross-section of the film to derive one-dimensional approximate equations. The continuity equation at steady state is

$$4\rho WHu = \rho Q = \text{constant} \qquad (2)$$

where Q is volumetric flow rate, u the mean velocity in the stretching direction x. The resulting momentum equation at steady state is

$$\frac{d}{dx}[WH\sigma_{xx}] = \rho WHu\frac{du}{dx} - WH\rho g - \kappa\frac{dR}{dx} \quad (3)$$

The right hand side of the above equation represents inertia, gravity and surface tension respectively. In the calculation of stress from the constitutive equation, it is assumed that the variation in the velocity component u over the cross-section is ignored.

2.1. Uniaxial elongational flow

If the melt drawn length between the die exit and the chill roll is large compared with the width and thickness of the slit die ($L >> W_o, H_o$) , then the sheet can be treated as a rod. Dynamics and kinematics of this process would be equivalent to the axisymmetric fiber spinning (Denn *et al.*, 1975; Schultz, 1987), and then a one-dimensional solution can be derived under this assumption. Viscous effect dominates the process for highly viscous polymers so that inertia, gravity and surface tension effects can be neglected. Then all of the terms on the right hand side of eq (3) are dropped, which after integration gives

$$4WH\sigma_{xx} = F = \text{constant} \quad (4)$$

Assuming that the fluid is Newtonian with a constant viscosity, the non-vanishing components of the stress tensor are

$$\sigma_{xx} = -p + 2\eta\frac{\partial u}{\partial x}$$
$$\sigma_{yy} = -p + 2\eta\frac{\partial v}{\partial y} \quad (5)$$
$$\sigma_{zz} = -p + 2\eta\frac{\partial w}{\partial z}$$

Here it is supposed that the local state of flow is a uniaxial elongation. Then, the following forms of the stress tensor are obtained after substituting eq (1) into eq (5).

$$\sigma_{xx} = -p + 2\eta\frac{du}{dx}, \quad \sigma_{yy} = \sigma_{zz} = -p - \eta\frac{du}{dx} \quad (6)$$

Since a total force in the x direction from the die exit to any position x is the applied tension F, the cross-sectional force balance gives $\sigma_{yy} = \sigma_{zz} = p_a$, where p_a is the ambient pressure. If the ambient pressure is taken to be zero, eq (6) gives

$$p = -\eta\frac{du}{dx}, \quad \sigma_{xx} = 3\eta\frac{du}{dx} \quad (7)$$

From eqs (2), (4) and (7), we find the following form of equation.

$$\frac{du}{dx} = \frac{uF}{3\eta Q} \quad (8)$$

Integrating eq (8) and applying relevant boundary conditions give

$$u = u_o\exp\left(\frac{x}{L}\ln Dr\right)$$
$$v = v_o\exp\left(\frac{x}{L}\ln Dr\right)\frac{y}{W_o} \quad (9)$$
$$w = w_o\exp\left(\frac{x}{L}\ln Dr\right)\frac{z}{H_o}$$

where the draw ratio Dr is defined as u_L / u_o , $\ln Dr = FL/3\eta Q$, and v_o and w_o are defined as $-u_o FW_o / 6\eta Q$ and $-u_o FH_o/6\eta Q$ respectively. Using the relation of $W/W_o = H/H_o$ from eq (2), the free surface profiles are expressed as follows.

$$W = W_o\exp\left(-\frac{xF}{6\eta Q}\right) = W_o\exp\left(-\frac{x}{2L}\ln Dr\right)$$

$$H = H_o\exp\left(-\frac{xF}{6\eta Q}\right) = H_o\exp\left(-\frac{x}{2L}\ln Dr\right) \quad (10)$$

2.2. Planar elongational flow

If the width of the sheet is much larger than the thickness and the melt drawn length, the flow field can be considered as planar elongation in the x and z directions. As a result, the flow can be regarded as two-dimensional and all steady flow quantities in sheet casting process are assumed to be independent of y. Beyond the die swell region it may be reasonable to assume that the relaxation process is complete and the variation in the z direction of u is much less significant than its variation in the x direction. It is thus possible to approximate $u(x,z)$ by $u(x)$. Yeow (1974) obtained an analytical steady state solution on the basis of these assumptions. With the above assumptions, the stress fields can be written as

$$\sigma_{xx} = -p + 2\eta\frac{du}{dx}, \quad \sigma_{yy} = -p, \quad \sigma_{zz} = -p - 2\eta\frac{du}{dx} \quad (11)$$

As in the case of uniaxial elongation, σ_{zz} remains constant in the flow field and becomes zero. Then,

$$p = -2\eta\frac{du}{dx}, \quad \sigma_{xx} = -4\eta\frac{du}{dx} \quad (12)$$

Solving eqs (2), (4) and (12) yields the following velocity fields and thickness profile,

$$u = u_o\exp\left(\frac{x}{L}\ln Dr\right)$$
$$w = w_o\exp\left(\frac{x}{L}\ln Dr\right)\frac{z}{H_o} \quad (13)$$
$$H = H_o\exp\left(-\frac{x}{L}\ln Dr\right)$$

where $w_o = -u_o FH_o / 4\eta Q$ in this case.

2.3. Mixed elongational flow

More general elongational flow should be considered in the analysis of sheet casting process because the flow is

neither purely uniaxial nor purely planar elongational. This mixed flow can also be based on the quasi-elongational approximation: the assumption of uniform velocity profiles across the sheet is made, in the same way as in the previous sections. If we assume $\dot{\varepsilon} = du/dx$, the stress components of the Newtonian fluid for the elongational flow are

$$\sigma_{xx} = -p + 2\eta\frac{\partial u}{\partial x}$$
$$\sigma_{yy} = -p - 2\eta(1-b)\frac{\partial u}{\partial x} \quad (14)$$
$$\sigma_{zz} = -p - 2\eta b\frac{\partial u}{\partial x}$$

If we let W and H depend only on the x direction, then eq (2) gives $WH = f(x)$. From momentum equations, it can be assumed that p is independent of y and z directions, so that the combination of eqs (4) and (14) gives

$$\frac{du}{dx} = \frac{F}{2\eta WH} + \frac{p}{2\eta} = g(x) \quad (15)$$

Previous results suggest to try

$$g(x) = A\ \exp\ (Bx) \quad (16)$$

Applying the boundary conditions of $u(0) = u_o$ and $u(L) = u_L$ on eq (15), the velocity fields are expressed as

$$u = u_o \exp\left(\frac{x}{L}\ln Dr\right)$$
$$v = v_o \exp\left(\frac{x}{L}\ln Dr\right)\frac{y}{W_o}$$
$$w = w_o \exp\left(\frac{x}{L}\ln Dr\right)\frac{z}{H_o} \quad (17)$$

where v_o and w_o are defined by $v_o = -(1 - b)u_o W_o(\ln Dr) / L$, $w_o = -bu_o H_o(\ln Dr) / L$. For steady flow, the kinematic condition on the free surface of the sheet requires $dH/du = w/u$ at $z = \pm H$ and $dW/dx = v/u$ at $y = \pm W$. These equations together with eqs (2) and (17) give

$$H = H_o \exp\left(-\frac{x}{L}b\ln Dr\right) \quad (18)$$
$$W = W_o \exp\left(-\frac{x}{L}(1-b)\ln Dr\right)$$

This is a simple extension of the results in the previous sections. The dimensionless velocity profiles at various values of the draw ratio are shown in Fig. 3. The dimensionless thickness profile H/H_o is a function of the dimensionless length x/L, the draw ratio Dr and the parameter b. The dimensionless thickness profiles are shown in Fig. 4 at the draw ratio of 10 and various values of the parameter b, where $b = 0.5$ corresponds to the uniaxial elongation and $b = 1$ to the planar elongation.

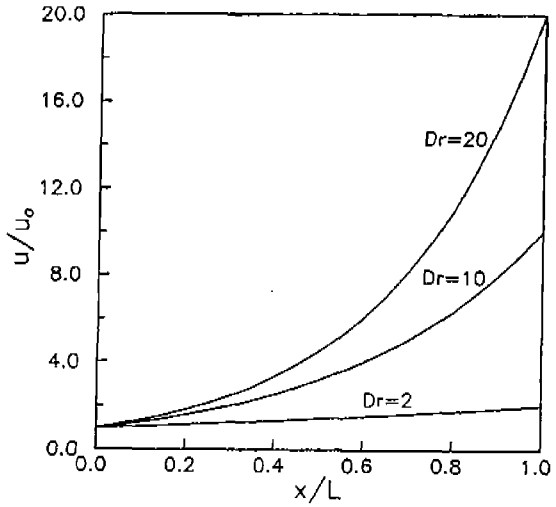

Fig. 3. Dimensionless velocity profiles as a function of dimensionless length at various draw ratios.

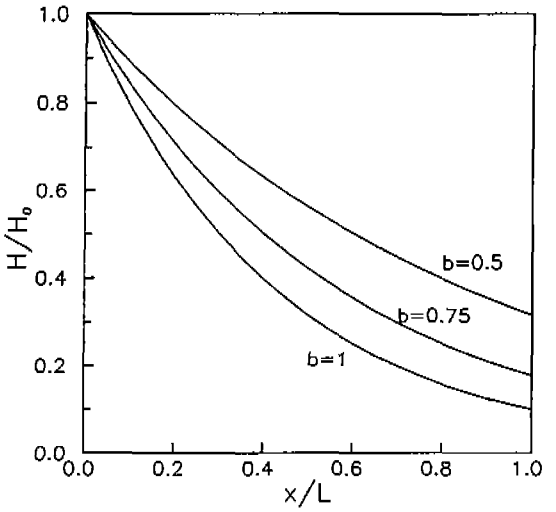

Fig. 4. Dimensionless velocity profiles as a function of dimensionless length at draw ratio of 10 and various values of parameter b.

3. Comparison with numerical solutions

The full three-dimensional numerical simulation of sheet casting process are carried out at several ratios of initial width to melt drawn length W_o/L of 2, 4, 5, 7 and 8 on the finite element meshes which are generated by POLYFLOW® and modified in the previous paper (MESH2 and MESH3 of Chae *et al.*, 2000). The flow kinematics at the low ratio of W_o/L comes close to that of the uniaxial elongational flow. If the ratio increases infinitely, the flow kinematics would approach to the planar elongational flow. The dimensionless velocity u/u_o and the thickness distribution H / H_o are shown in Figs. 5-10 at various values of W_o/L and draw ratios along with the dimensionless stretching length x / L. In these figures, the solid lines indicate solutions

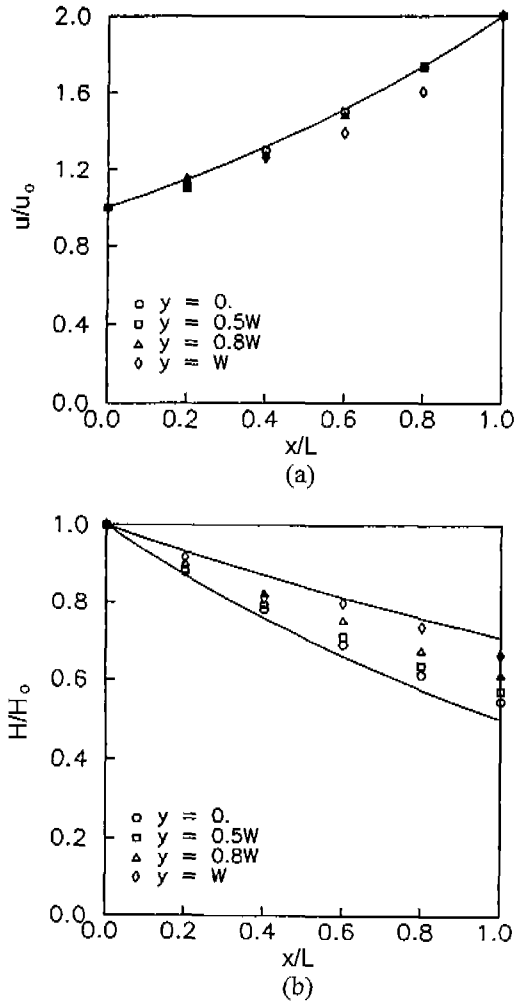

Fig. 5. Dimensionless velocity profiles (a) and thickness profiles (b) along dimensionless length when $W_o/L = 2$ and $Dr = 2$.

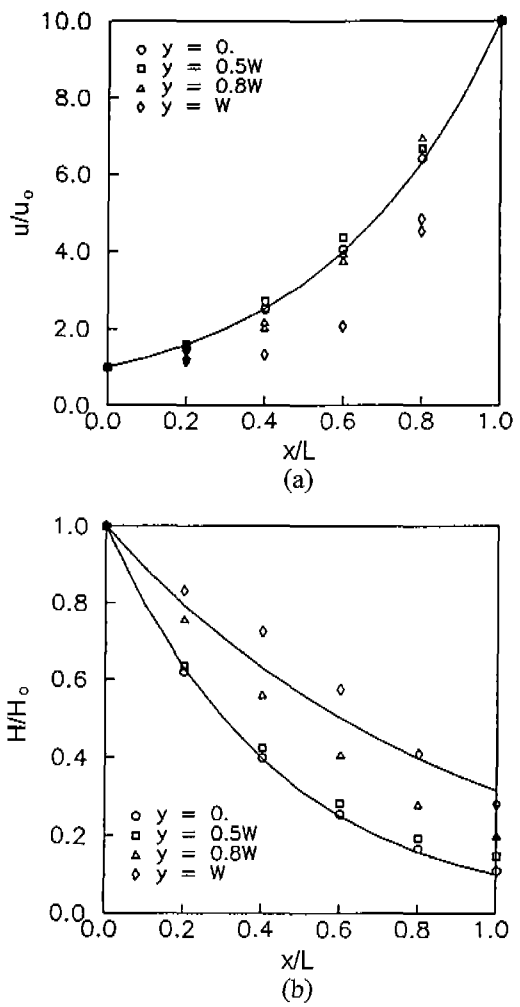

Fig. 6. Dimensionless velocity profiles (a) and thickness profiles (b) along dimensionless length when $W_o/L = 2$ and $Dr = 10$.

obtained from the one-dimensional approximations, eqs (17) and (18), and various shapes of symbols indicate the solutions obtained from the full three-dimensional numerical simulations. These figures display the dimensionless velocity and thickness distributions at the different positions of y, where $y = 0$ represents the center line and $y = W$ the free surface line. The profiles of the dimensionless velocity at $W_o/L = 2$ are shown in Figs. 5(a) and 6(a). As the draw ratio increases, the numerical solution of the dimensionless velocity departs from the analytical solution: the farther away from the central region of the sheet it is, the more it deviates. The thickness distributions at $W_o/L = 2$ can be seen in Figs. 5(b) and 6(b), where the upper solid line corresponds to uniaxial elongation ($b = 0.5$) and the lower solid line corresponds to planar elongation ($b = 1$). Analogous result patterns for $W_o/L = 5$ and 8 are shown in Figs. 7-10. It is observed that the thickness distribution comes close to the planar elongational approximation near the central region and approaches the uniaxial elongational approximation near the edge region. The range of the dimensionless velocity, for which the one-dimensional approximation is valid, extends as the draw ratio decreases under the same value of W_o/L.

For the dimensionless thickness profile, the central region which satisfies the planar elongational approximation is much broader in the case of large values of W_o/L. As can be seen in Figs. 5-10, it is thought that the off-centered non-planar elongation zone is rather narrow compared with the overall flow field as the value of W_o/L increases. When a position is sufficiently away from the edge region, it is commonly known that the velocity and the thickness profile of the sheet become relatively independent of y, so that the flow is nearly planar elongational. Thus, by comparing one-dimensional solutions with numerical soluions as represented in Figs. 5-10, it is now possible to determine the part of the domain in which the flow field can be satisfied by the one-dimensional approximation. When W_o/L is 5 (Figs. 7 and 8), the dimensionless velocity and thickness distributions begin to deviate from the analytical solutions

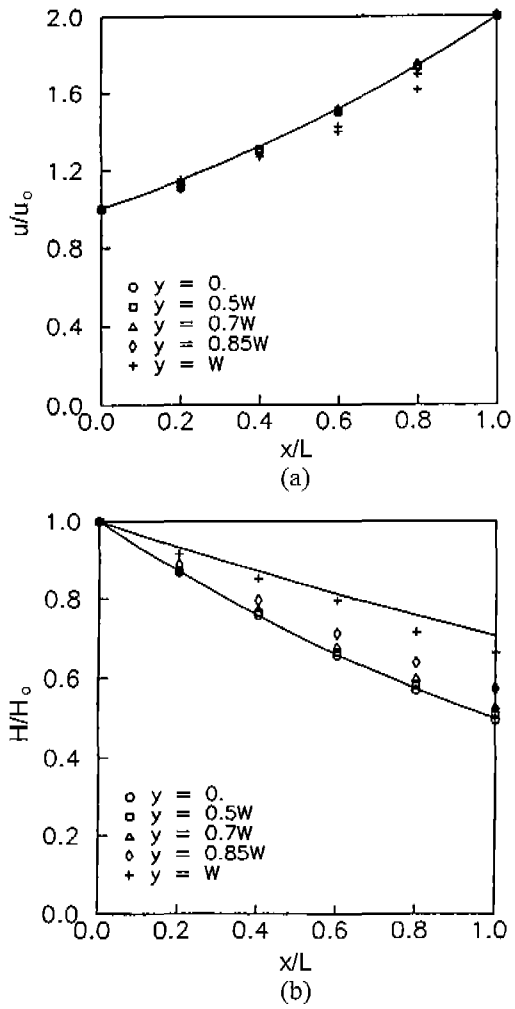

Fig. 7. Dimensionless velocity profiles (a) and thickness profiles (b) along dimensionless length when $W_o/L = 5$ and $Dr = 2$.

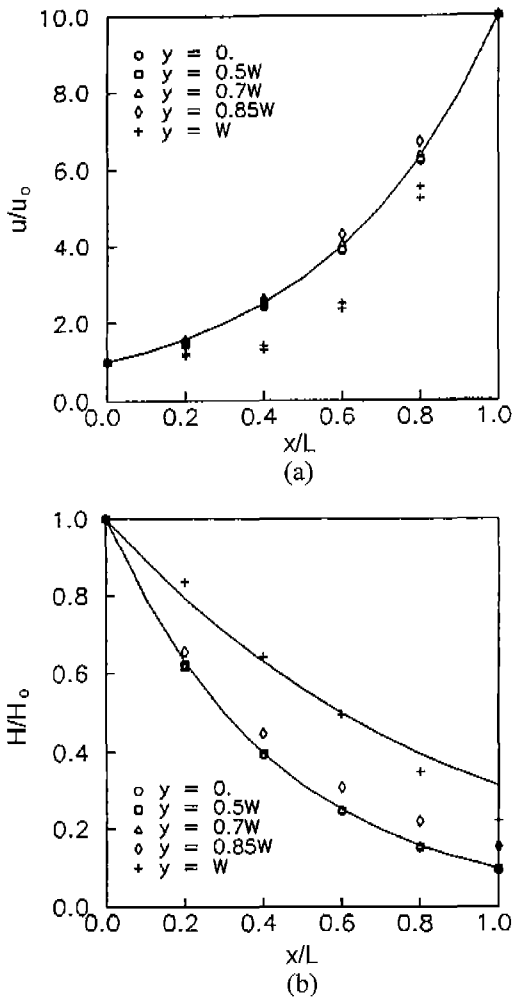

Fig. 8. Dimensionless velocity profiles (a) and thickness profiles (b) along dimensionless length when $W_o/L = 5$ and $Dr = 10$.

along the dimensionless length after $y = 0.5$W and the range of width which the planar elongation may hold is about 0.5W. This may explain the validity range of one-dimensional models in the prediction of sheet profile. The range of width which satisfies the planar elongational approximation for various ratios of W_o/L is shown in Fig. 11, and within this range no edge effects are likely to be observed. In this figure, the solid line is calculated by the extrapolation of five data points, although the dimensionless velocity and thickness profiles along the dimensionless length for $W_o/L = 4$ and 7 are not shown in this paper. Since the edge bead and neck-in phenomena in the edge region cannot be described by one-dimensional analysis alone, the prediction of sheet profile requires three-dimensional numerical simulation inevitably where necessary.

4. Coupled solutions

The approach proposed in this study to predict sheet profile is based on the observation that there exists a significant part of the domain whose flow kinematics can be described by the planar elongational flow. This implies that instead of simulating the full domain by three-dimensional calculations one-dimensional approximation can be replaced on the part of the domain where it is valid. Thus, the prediction range of sheet profile can be extended to the practical dimension of processing and the computation time can be saved using this coupled approach.

Two results are compared in the case of $W_o/L = 5$: the full numerical simulation which solves the entire domain of the sheet by three-dimensional calculations, and the coupled numerical simulation which solves the part of entire domain where the one-dimensional approximation is not valid. As seen in Fig. 11, it can be regarded that the range of width from $y = 0$ to $y = 0.5$W satisfies the one-dimensional approximation for $W_o/L = 5$. Then, the resultant one-dimensional approximation can be introduced as a part of the boundary conditions to simulate the flow behavior of

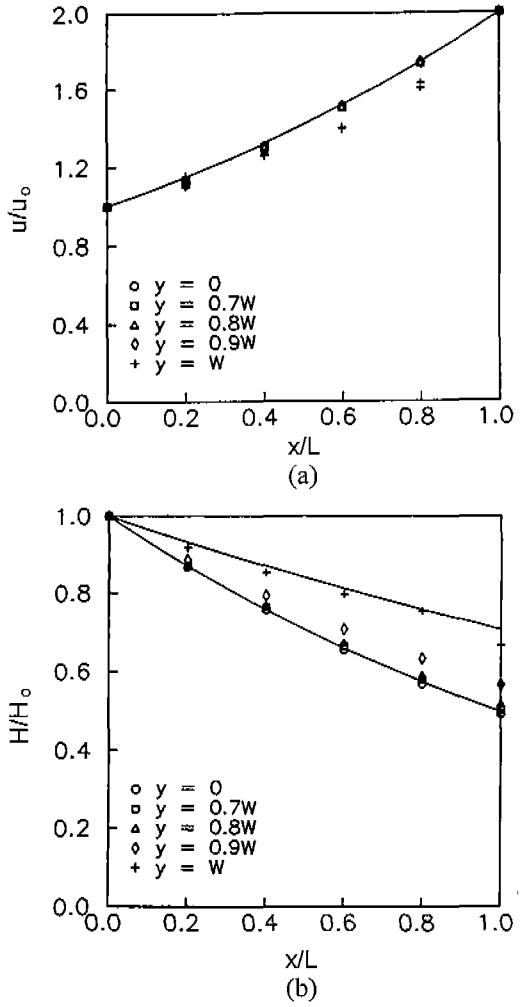

Fig. 9. Dimensionless velocity profiles (a) and thickness profiles (b) along dimensionless length when $W_o/L = 8$ and $Dr = 2$.

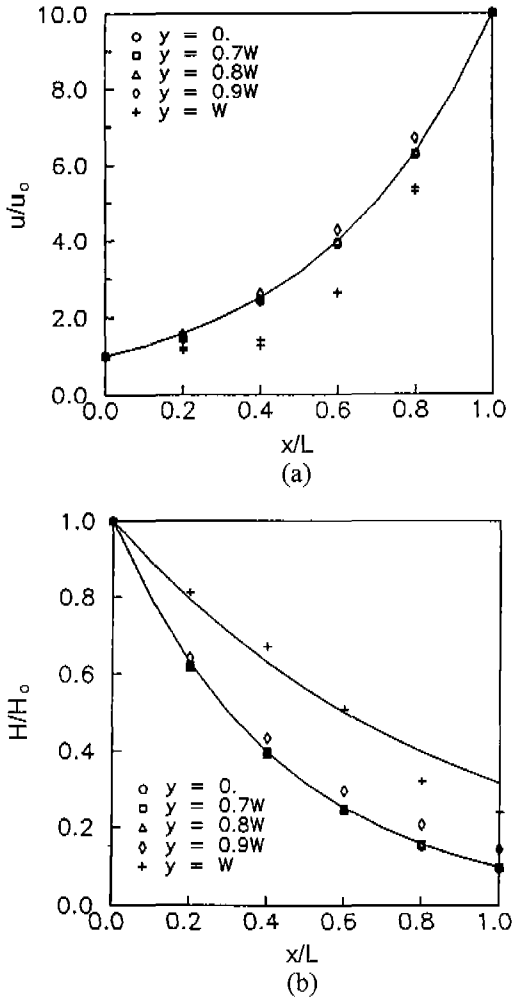

Fig. 10. Dimensionless velocity profiles (a) and thickness profiles (b) along dimensionless length when $W_o/L = 8$ and $Dr = 10$.

sheet casting process as shown in Fig. 12. Final sheet profiles at the chill roll are plotted together in Fig. 13 for $Dr = 2$ and 6 from which one can easily notice a similarity of two methods. In this figure, the dashed line represents the full numerical solution of the entire domain and the solid line with symbols represents the coupled solution of the partial domain. Here, the full numerical solution is obtained on MESH2 (195 elements) and the coupled solution on the test mesh (150 elements). From the comparison of two results, a quarter of the computing time is saved with a coupled approach. If two meshes have the same refinement on the domain of interest, the computing time might be further reduced. As seen in Fig. 13, the mutual agreement of both results evidently shows the basic validity of the coupled approach which requires less computing time for the prediction of sheet profile in sheet casting process. It is also expected that, compared with the full three-dimensional simulation, the computing time required for the three-dimensional numerical simulation by the

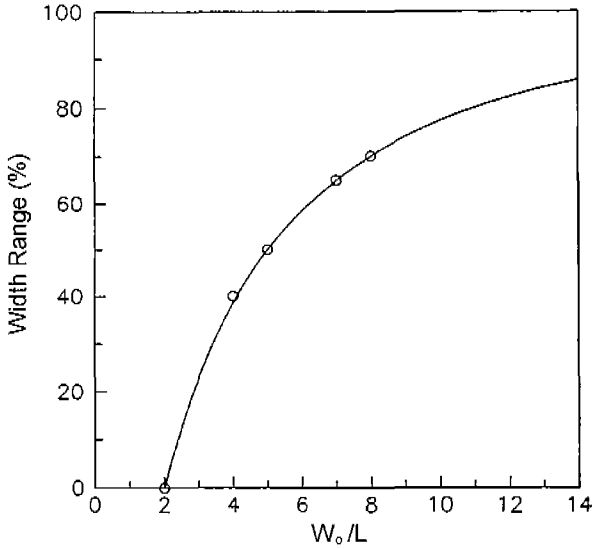

Fig. 11. Width range in which one-dimensional approximation is valid as a function of W_o/L.

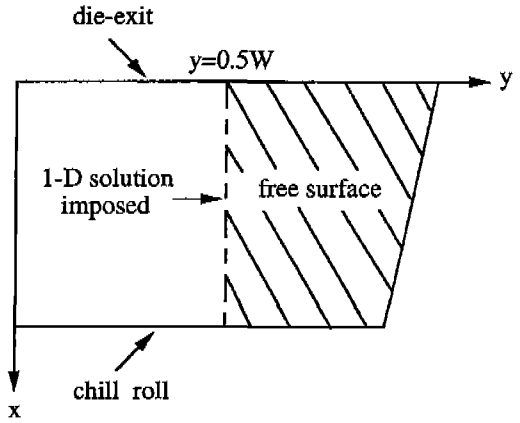

Fig. 12. Imposition of one-dimensional analytical solution into boundary condition of three-dimensional numerical simulation.

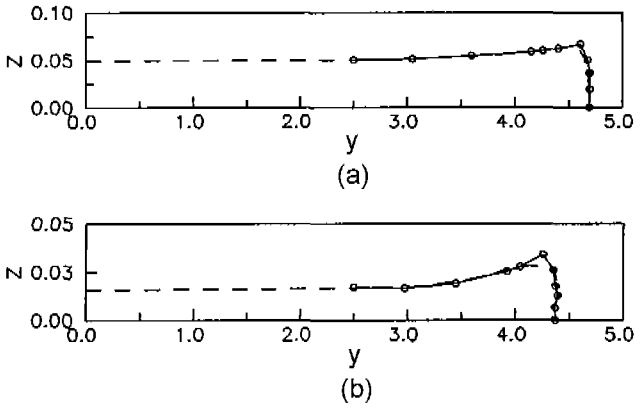

Fig. 13. Comparison of coupled numerical solution (—○—) with full three-dimensional numerical solution (– –) : (a) $Dr = 2$, (b) $Dr = 6$.

coupled approach can be saved more efficiently as the value of W_o / L becomes larger.

5. Conclusions

A coupled approach to predict sheet profile in sheet casting process is proposed which combines the one-dimensional analytical solution and the three-dimensional numerical simulation. This approach decomposes the flow domain into two partial subdomains comprised of the central region where the planar elongational flow dominates and the other region where the edge effect cannot be ignored. Coupled solution made up of the combination of the analytical approximation of the central region followed by the numerical simulation of the edge region shows good agreement with the full three-dimensional numerical simulation on the entire domain of interest. From the results so far concerned, the coupled approach proposed in this study may have provided flexibility to accomodate a wide range of die sizes in sheet casting process with less computing time. Since the experimental investigations of PET casting are in progress, their comparison with the full three-dimensional numerical simulation and the coupled solution of analytical and numerical methods will be reported in subsequent papers.

Acknowledgement

The authors wish to acknowledge the Korean Science and Engineering Foundation (KOSEF) for the financial support through the Applied Rheology Center, an official engineering research center (ERC) in Korea.

Nomenclature

b	: choice parameter for the type of elongational flows
Dr	: draw ratio
F	: applied tension
H	: half thickness of the sheet
H_o	: initial half thickness of the sheet
L	: melt drawn length
p	: pressure
p_a	: ambient pressure
Q	: volumetric flow rate
R	: total radius of curvature
u_L	: take-up velocity
u_o	: die-exit velocity
u,v,w	: velocity components in x, y, z directions
W	: half width of the sheet
W_o	: initial half width of the sheet

Greek letters

$\dot{\varepsilon}$	: elongation rate
η	: viscosity
κ	: surface tension coefficient
ρ	: density
σ_{ij}	: ij-component of total stress tensor

References

Bird, R. B., R. C. Armstrong and O. Hassager, 1987, *Dynamics of Polymeric Liquids, Vol. 1. Fluid Mechanics*, 2nd ed., John Wiley and Sons, New York, 101.

Canning, K. and A. Co, 2001, Edge effects in film casting of molten polymers, *J. Plastic Film and Sheeting* **16**, 188.

Chae, K. S., M. H. Lee, S. J. Lee and S. J. Lee, 2000, Three-dimensional numerical simulation for the prediction of product shape in sheet casting process, *Korea-Australia Rheol. J.* **12**, 107.

Debbaut, B. and J. M. Marchal, 1995, Viscoelastic effects in film casting, *Z. Angew Math. Phys.* **46**, 679.

Denn, M. M., C. J. S. Petrie and P. Avenas, 1975, Mechanics of steady spinning of a viscoelastic liquid, *AIChE J.* **21**, 791.

d'Halewyn, S., J. F. Agassant and Y. Demay, 1990, Numerical simulation of the cast film process, *Polym. Eng. Sci.* **30**, 335.

Pearson, J. R. A. and M. A. Matovich, 1969, Spinning a molten threadline: stability, *Ind. Eng. Chem. Fund.* **8**, 605.

Schultz, W. W., 1987, Slender viscoelastic fiber flow, *J. Rheol.* **31**, 733.

Smith, S. and D. Stolle, 1999, Simulation of draw resonance in film casting using a material description of motion, *ANTEC '99*, 255.

Song, K. S., 1993, Two dimensional numerical study on film casting process," MS thesis, Seoul National University, Korea.

Werner, E., S. Janocha, M. J. Hopper and K. J. Mackenzie, 1988, in *Encyclopedia of Polymer Science and Engineering*, ed. by H. F. Mark *et al.*, Vol. 12, Wiley-Interscience, New York, 193.

Yeow, Y. L., 1974, On the stability of extending films: A model for the film casting process, *J. Fluid Mech.* **66**, 613.